Isotope effect in the spin response of aluminum tris(8-hydroxyquinoline) based devices

Tho D. Nguyen,[1] T. P. Basel,[1] Y.-J. Pu,[2] X-G. Li,[3] E. Ehrenfreund,[1,4] and Z. V. Vardeny[1,*]

[1]*Department of Physics and Astronomy, University of Utah, Salt Lake City, Utah 84112, USA*

[2]*Department of Organic Device Engineering, Yamagata University, Yonezawa, 992-8510 Japan*

[3]*Hefei National Laboratory for Physical Sciences at Microscale, Department of Physics, University of Science and Technology of China, Hefei 230026, China*

[4]*Department of Physics, Technion-Israel Institute of Technology, Haifa 32000, Israel*

(Received 6 March 2012; published 20 June 2012)

We studied the spin response of various magnetic field effects and magnetotransport in both protonated and deuterated aluminum tris(8-hydroxyquinoline) [Alq_3]-based organic light emitting diodes and spin-valve devices. Both conductivity-detected magnetic resonance in diodes and magnetoresistance in spin valves show substantial isotope dependence pointing to the importance of the hyperfine interaction (HFI) in the spin response of spin $\frac{1}{2}$ charge polarons in Alq_3. In addition, the low field ($B < 20$ mT) magnetoelectroluminescence (MEL) response is also isotope sensitive, showing that HFI-induced spin mixing of polaron-pairs spin sublevels dominates this response too. However, the magnetoconductance (MC) response was found to be much less sensitive to isotope exchange at low fields, in agreement with previous studies. The disparity between the isotope sensitivity of MC and MEL responses in Alq_3 indicates that the HFI in the MC response is overwhelmed by an isotope independent spin mixing mechanism. We propose that collisions of spin $\frac{1}{2}$ carriers—with triplet species such as polaron pairs may be the main spin mixing mechanism in the low field MC response in Alq_3 diodes.

DOI: 10.1103/PhysRevB.85.245437 PACS number(s): 72.25.−b, 85.75.−d, 72.80.Le

I. INTRODUCTION

Aluminum tris(8-hydroxyquinoline) (Alq_3) [see molecular structure in Fig. 1(a) inset] is a common active molecular layer used in organic light emitting devices (OLED), due to its efficient electroluminescence (EL) emission and high electron mobility.[1–3] It is thus not surprising that magnetic field effects (MFE) in Alq_3-based OLED devices such as magnetoelectroluminescence (MEL) and magnetoconductance (MC) have been extensively studied in the last few years.[4–10] As a result, several basic models were originally proposed to explain the obtained magnetic-field effect response, MFE(B). Basically, all models agree that the underlying mechanism for the MFE is the magnetic field dependence of spin sublevel mixing; but there is no consensus as to the basic excitation species in which the spin mixing occurs. The competing models include: (i) spin mixing in oppositely charged polaron pairs (PP) and in pairs of same-charge polarons (or bipolarons, BP) by the hyperfine interaction (HFI);[4,6,11,12] (ii) spin mixing within triplet-triplet annihilation (TTA) process;[7] and (iii) spin mixing during the process of triplet exciton quenching by spin $\frac{1}{2}$ charge polarons.[8] Importantly, the HFI-based models should differ substantially from the other models in the response to isotope exchange in the Alq_3 molecule active layer, where all hydrogen atoms (nuclear spin $I_H = \frac{1}{2}$, nuclear g factor $g_H = 5.586$) are exchanged by deuterium atoms ($I_D = 1$, $g_D/g_H = 0.154$). This should occur since the HFI constant a_{HF} scales with the nuclear g factor,[13] whereas the other proposed interactions are mostly isotope insensitive. Consequently, the isotope exchange effect on the MFE(B) response in Alq_3-based OLED was recently studied to scrutinize the proposed spin-mixing models.[9,14] It was concluded that the MFE in Alq_3-based OLED is not dominated by PP or BP species since it was found that the HFI does not play a major role in determining the MC(B) and MEL(B) responses. This conclusion is surprising because similar MFE measurements in devices based on a common π-conjugated polymer, namely poly(dioctyloxy) phenyl vinylene (DOO-PPV), have shown a substantial isotope effect.[15,16] It is thus important to investigate in more detail the influence of the isotope exchange on the MFE and magnetotransport in Alq_3-based devices, in order to identify the underlying spin-exchange mechanisms.

In this work we present a detailed study of the MFE response and magnetotransport in protonated (H-) and deuterated (D-) Alq_3-based OLED and spin-related devices. These studies include spin $\frac{1}{2}$ conductivity detected magnetic resonance (CDMR) in organic diodes, magnetoresistance (MR_{SV}) in organic spin valves (OSV), and MC and MEL responses in OLED devices. We found that the spin $\frac{1}{2}$ CDMR is *isotope sensitive*. It shows a narrower resonant line in D-Alq_3 compared to H-Alq_3 devices, and therefore the polaron excitation in Alq_3 is definitely influenced by the HFI. This indicates that spin-related effects based on polaron excitations should be isotope sensitive in this molecule. Indeed we measured superior MR_{SV} response in D-Alq_3 OSV devices, which indicates larger spin diffusion length due to the reduced HFI with the deuterium isotope nuclei. Moreover a clear sizable isotope dependent MEL(B) response in OLED was also observed at low fields ($B < \sim 20$ mT), showing that HFI-induced spin mixing of polaron-pairs spin sublevels plays a crucial role also in determining the MEL response in Alq_3-based OLED. However the MC(B) response at low fields was found to be much less sensitive to the isotope exchange. In addition, at high fields both MEL(B) and MC(B) responses are isotope insensitive, and do not show the expected HFI-related saturation up to $B \sim 250$ mT. These puzzling MFE characteristic properties can be understood taking into consideration that in addition to the HFI in PP (or BP) species, other spin-mixing mechanisms also participate in determining the MFE in Alq_3 diodes. We propose that an isotope independent collisions of spin $\frac{1}{2}$ polarons with spin triplet species (e.g., PP, BP, or TE) is the main spin mixing mechanism responsible for the low field MC(B) response.

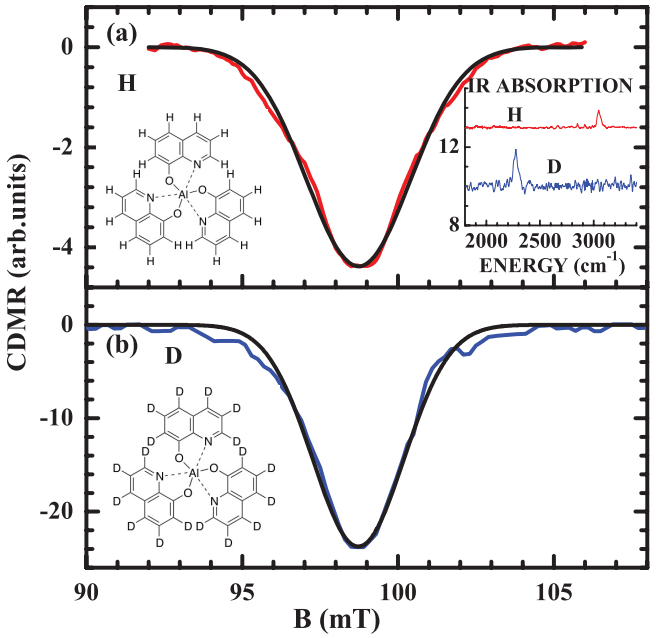

FIG. 1. (Color online) Spin $\frac{1}{2}$ CDMR of (a) H_{18}-Alq_3 (red line) and (b) D_{18}-Alq_3 (blue line) measured at ∼3 GHz and 10 K; the FWHM are 3.94 and 3.46 mT, respectively. The black lines are fits using inhomogeneous broadened (Gaussian profile, FWHM = 3.4 mT) hyperfine split resonance, with $a_{HF} = 3$ and 0.46 mT, respectively, for H-Alq_3 and D-Alq_3. The molecules' chemical structures are shown in the left insets. The right inset in (a) shows the molecules' infrared absorption spectra (red for H-Alq_3 and blue for D-Alq_3), having a red-shifted C-D stretching mode that occurs upon deuteration; namely $\nu_{CH} = 3050\ cm^{-1}$ and $\nu_{DH} = 2276\ cm^{-1}$.

II. EXPERIMENT

The active layers in our spin-related device studies were the following two Alq_3 isotopes: $H_{18}Alq_3$ and $D_{18}Alq_3$, where all the hydrogen atoms in H-Alq_3 were replaced by deuterium.[17] Figures 1(a) and 1(b) (left insets) show the Alq_3 molecular structure and the H (D) atoms positions. We used both NMR spectroscopy and infrared (IR) absorption to verify that all hydrogen atoms were replaced by deuterium atoms in the D-Alq_3 molecules. The IR absorption spectrum of the two Alq_3 isotopes in the range of the C-H stretching vibration ν_{CH} shows a deuteration related shift according to the expected mass ratio [Fig. 1(a), right inset]. We measured $\nu_{CH} = 3050\ cm^{-1}$ and $\nu_{DH} = 2276\ cm^{-1}$; and thus their ratio is within 2% of the square root C-D/C-H reduced mass ratio. In particular the lack of an absorption band at 3050 cm^{-1} in the IR absorption spectrum of D-Alq_3 indicates that there are little or no hydrogen atoms present in this molecule.

The Alq_3-based OLED devices were fabricated using glass substrates coated with 40 nm of indium-tin-oxide (ITO) that were purchased from Delta Technologies. The conducting polymer poly(3,4-ethylenedioxythiophene)-poly(styrenesulfonate) (PEDOT) [H C Starck] was spin-coated onto the ITO used as the anode. The H-Alq_3 (D-Alq_3) that was synthesized in house was then thermally evaporated onto the bottom electrode. Subsequently a Ca cathode with an Al capping layer was deposited by thermal evaporation onto of the Alq_3 thin film. The complete device structure configuration was ITO/PEDOT(30 nm)/Alq_3(70 nm)/Ca(20 nm)/Al(50 nm) having an active area of ∼2 × 2 mm^2.

For the CDMR measurements the Alq_3-based OLED devices were placed in an *S*-band (∼3 GHz) microwave (MW) cavity in a cryostat at 10 K equipped with MW throughput cables; the MW radiation was provided by a Gunn diode that delivered up to $P_{MW} \sim 0.1$ W power. The cryostat was placed inside a liquid He cooled superconducting coil that provided magnetic fields up to 3 T, applied perpendicular to the device substrate. P_{MW} was modulated at frequency $f \sim 200$ Hz and the change ΔI in the current I was monitored using a lock-in amplifier at f. The magnetic field B was swept while monitoring ΔI. Resonance condition for spin $\frac{1}{2}$ and $g \approx 2$ occurs when the MW photon energy is equal to the energy difference between the two Zeeman split spin sublevels at $B \sim 0.1$ T. For comparing the resonance profile of the two Alq_3 isotopes we measured $\Delta I(B)/I$ under identical conditions such as device structure, applied voltage, temperature, and microwave power.

For the MEL and MC measurements, the Alq_3-based OLED devices were transferred to an optical cryostat with variable temperature that was placed in between the two pole pieces of an electromagnet that produced B in the range ±0.3 T with 10^{-5} T resolution; in all measurements B was determined by a calibrated magnetometer. The devices were driven at constant voltage V or constant current I using a Keithley 236 apparatus; whereas the EL intensity was measured by a Si photodetector, while sweeping B in both positive and negative directions. The MC(B) [MEL(B)] is defined by the relation $\Delta I(B)/I(0)$ [ΔEL(B)/EL(0)], and is positively defined when I increases with B.

The OSV devices were fabricated using the half-metal $La_{0.67}Sr_{0.33}MnO_3$ (LSMO) as the spin injector FM anode. The Alq_3, Co, and Al layers were successively thermally evaporated onto the LSMO electrode, similar to the OLED fabrication described above. The OSV device structure was LSMO(200 nm)/Alq_3(40 nm)/Co(6 nm)/Al(50 nm) with an active area typically of ∼0.2 × 0.4 mm^2. All thermal evaporations were done in a high vacuum environment (5 × 10^{-7} mbar). The film thickness was measured using thickness profilometry (KLA Tencor). The OSV magnetoresistance response MR_{SV} was measured in a closed-cycle refrigerator at temperatures T in the range 10–300 K using the "four probe" method in a constant current mode using a Keithley 236 apparatus, while varying the external in-plane magnetic field. The magnetization properties of the FM electrodes were measured by the magneto-optic Kerr effect (MOKE); from these measurements we determined typical low temperature (10 K) coercive fields of the unassembled electrodes as $B_{c1} \sim 4.5$ mT and $B_{c2} \sim 15$ mT for the LSMO and Co electrodes, respectively.

III. RESULTS AND ANALYSIS

A. Conductivity detected magnetic resonance

The CDMR spectra of H- and D-Alq_3 OLED devices [Figs. 1(a) and 1(b), respectively] is negative under magnetic resonance conditions. CDMR in π-conjugated systems measures changes in the polaron pair (PP) density[18] under

resonance conditions. Therefore the CDMR spectra in Fig. 1 show the effect of isotope exchange on the PP spin density. The resonance line of H-Alq_3 is inhomogeneously broadened;[16] the full width at half maximum (FWHM) is ∼3.94 mT for the H-Alq_3 and 3.54 mT for the D-Alq_3, substantially larger than the FWHM (<2 mT) obtained in spin $\frac{1}{2}$ CDMR of devices based on DOO-PPV polymer.[16] Using the same model presented earlier in Ref. 16, we show fits (black solid lines in Fig. 1) to the measured CDMR line shapes of the H- and D-Alq_3 devices using an inhomogeneously broadened hyperfine split resonance line with $a_{HF} = 3$ and 0.46 mT, respectively. The smaller FWHM measured for the D-Alq_3 device is a strong indication that the HFI indeed plays an important role in the PP spin dynamics in this molecule.

B. Magnetoresistance in organic spin valves

Further evidence for the HFI importance for spin $\frac{1}{2}$ polarons in Alq_3 is revealed in the magnetoresistance (MR_{SV}) measurements in OSV devices based on D- and H-Alq_3 interlayer (Fig. 2). It is seen that MR_{SV} of D-Alq_3 [Fig. 2(b)] is three times larger than that of H-Alq_3 [Fig. 2(a)]. The superior MR response of the D-Alq_3 OSV is maintained at various voltages [Fig. 2(c)], showing that the spin diffusion length λ_S in the deuterated spin valve is substantially larger than that in the hydrogenated device. λ_S in OSV devices increases with the spin relaxation time τ_s: (a) for carrier diffusion motion $\lambda_s = \sqrt{D\tau_s}$, where D is the carrier diffusion constant which is proportional to the carrier mobility μ via the Einstein relation; (b) for carrier drift motion in an applied electric field F, $\lambda_s = \mu F \tau_s$. Assuming that carrier mobility is not influenced by the isotope exchange, we conjecture that the larger λ_S obtained in D-Alq_3 OSV is due to longer spin $\frac{1}{2}$ relaxation time; and this also points to the importance of the HFI in the spin $\frac{1}{2}$ polaron transport in Alq_3 devices.

C. Magnetoelectroluminescence in OLEDs

1. The low field regime

The MEL(B) response of H- and D-Alq_3 OLED are shown with various field resolution in Figs. 3(a)–3(c); a clear isotope dependent response can be seen. First, the width ΔB of the MEL(B) response in H-Alq_3 device is ∼40% larger than that in D-Alq_3 [Figs. 3(b) and 3(a) inset]. This observation is at variance with an earlier study in which much smaller dependence on the isotope exchange was reported.[9,14] Second, the MEL(B) response shows another feature at low fields ($B < \sim 2$ mT) [Fig. 3(c)]: as $|B|$ is varied from $B = 0$ MEL(B) is negative, reaches a minimum value at $|B| = B_m$, then monotonically increases thereafter, including a zero crossing. We clearly see that B_m is isotope dependent: $B_m = 0.2$ mT for D-Alq_3 and 0.4 mT for H-Alq_3. Similar features, dubbed ultrasmall magnetic field effect (USMFE) were previously obtained in DOO-PPV based OLEDs, where the isotope dependence was shown to originate from the HFI in PP species.[15,16] We therefore conclude that the HFI in PP species plays a dominant role also in the low-field MEL response in Alq_3 devices. We note however, that the obtained ratios $B_m(\mathrm{H})/B_m(D) \approx 2$ and $\Delta B(\mathrm{H})/\Delta B(\mathrm{D}) \approx 1.4$ in Alq_3 OLEDs are about 30%–40% smaller than those measured in DOO-PPV isotopes.[16] This observation indicates that in addition to the HFI, other interactions that are isotope insensitive have to be taken into account for explaining the detailed MEL response in Alq_3.[14] An in-depth discussion of the isotope effect in the low field MEL Alq_3 response is presented in Secs. IV and V below.

2. The high field regime

At higher fields ($|B| \sim$ 50–250 mT) the MEL response does not level off; instead it continues to increase, in contrast to what is expected for MFE response governed by the HFI.[11,16] This characteristic behavior indicates that a different mechanism is dominant for the high field response of both MEL and MC.

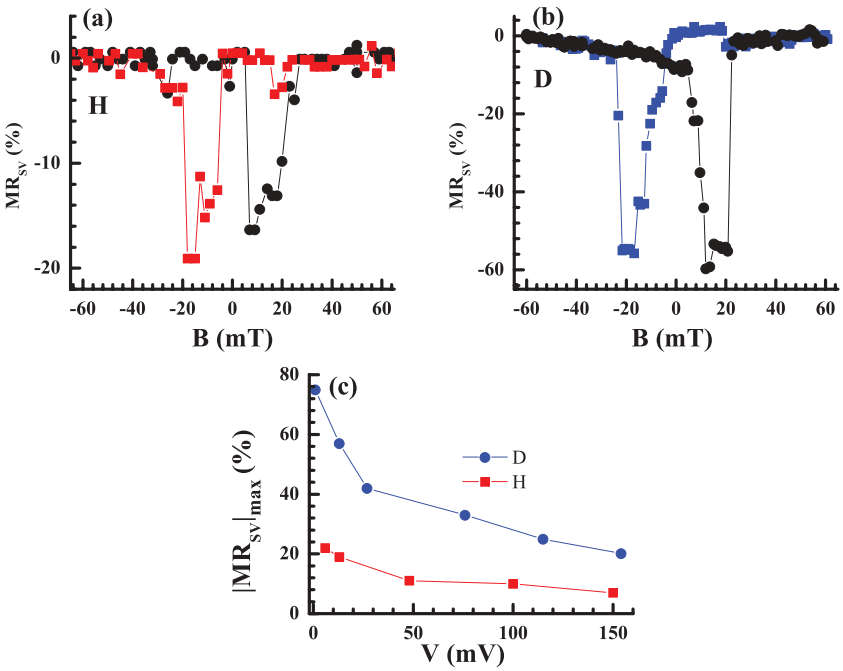

FIG. 2. (Color online) The spin valve related magnetoresistance, $MR_{SV}(B)$ response of two 40 nm thick OSV devices based on (a) H-Alq_3 and (b) D-Alq_3 for up (black) and down (colored) B sweeps, measured at $V = 12$ mV and $T = 10$ K. (c) Bias voltage dependence of $|MR_{SV}|_{max}$ for H-Alq_3 (red squares) and D-Alq_3 (blue circles).

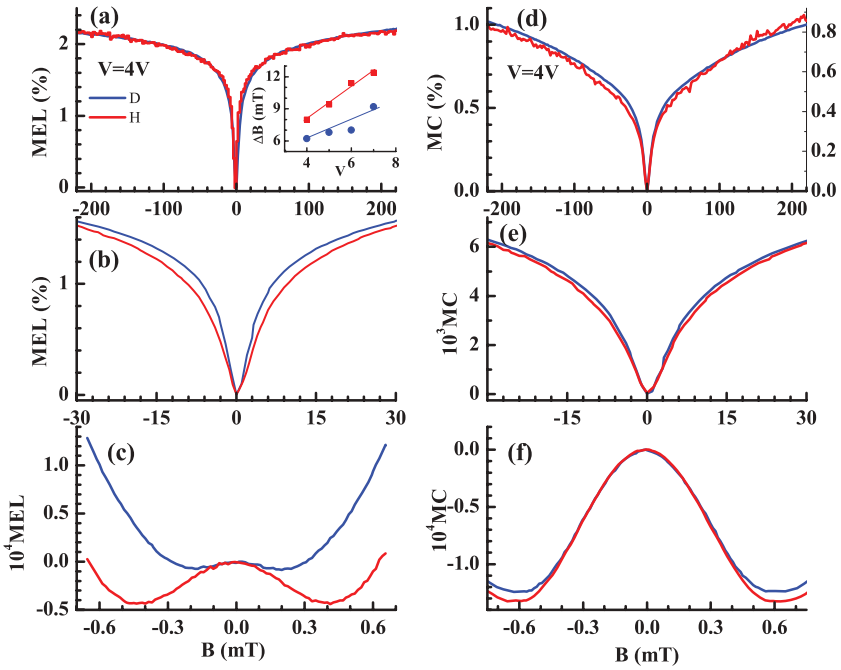

FIG. 3. (Color online) (a)–(c) MEL(B) response of OLEDs based on H-Alq_3 (red line) and D-Alq_3 (blue line) measured at room temperature and bias $V = 4$ V, plotted at three *different B scales*. The D-Alq_3 response was normalized to that of H-Alq_3 at $B \sim 250$ mT. Inset in (a): The full width, ΔB, measured at MEL = 0.8% plotted vs V for H-Alq_3 (red) and D-Alq_3 (blue). (d)–(f) Same as in (a)–(c) but for the MC(B) responses measured on the same devices.

Alq_3 is known to have phosphorescence emission from triplet excitons (TE) and delayed fluorescence caused by triplet-triplet-annihilation.[19] Therefore it is likely that TE are involved in the MFE response at intermediate high fields, via high order recombination. In order to examine this hypothesis we exposed the Alq_3-based OLED devices to oxygen atmosphere, which is known to quench TE species.[20] Figure 4 shows the MEL(B) response of oxygen-exposed OLED devices of both Alq_3 isotopes. The MEL response is similar to that shown in Fig. 3, but with much clearer difference between the responses of the two isotopes. The MEL width of H-Alq_3 OLED defined in Fig. 4 is now two times larger than that of D-Alq_3 OLED. This shows that the intermediate high field MEL response obtained in unexposed devices comes from TE, which is insensitive to isotope exchange. When this component is quenched by exposure to oxygen then the HFI-dominated component prevails, and consequently the isotope dependent response becomes clearer.

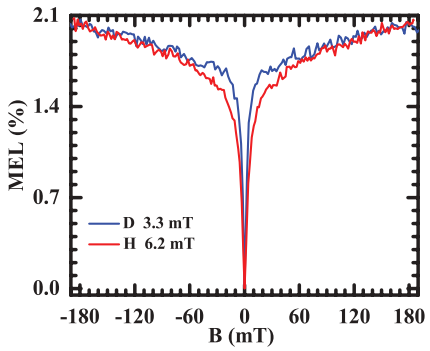

FIG. 4. (Color online) MEL(B) response of OLEDs based on H- and D-Alq_3 saturate exposed to oxygen, measured at $V = 4$ V and room temperature. The full width ΔB measured at MEL = 1% is 12.4 mT (6.6 mT) for the H-Alq_3 (D-Alq_3) device. The response of D-Alq_3 was normalized to that of H-Alq_3 at $B = 200$ mT.

D. Magnetoconductance in OLEDs

Figures 3(d)–3(f) show the MC(B) response measured on the same OLED devices in which the MEL(B) responses were measured [Figs. 3(a)–3(c)]. Although the MC(B) responses seem to be similar to MEL(B), the isotope dependence is different. Figure 3(f) shows that at low fields B_m(H) $\approx$ B_m(D) ($\approx$0.6 mT) for the MC response, whereas the ratio $B_m(\mathrm{H})/B_m(\mathrm{D}) \approx 2$ for the MEL response. Also when the isotope dependent MC responses are normalized at the maximum measured field of $B_{\max} \approx 220$ mT [Fig. 3(e)], then the two responses appear to be much less isotope sensitive than the MEL responses [Fig. 3(a)]. This indicates that a mechanism *other than the HFI* dominates the MC(B) response at low fields ($|B| <$ 20–30 mT).

IV. DISCUSSION

A. The polaron-pair mechanism: Isotope sensitive MEL response

As argued in Sec. III the low field MEL(B) response should be described by the PP mechanism, with the HFI as the main spin mixing process. Since the measured MEL(B) response shows significant isotope effect, the spin-orbit coupling and/or the exchange interaction contributions are relatively small here. For completeness we now present the PP mechanism model which is based on the time evolution of the PP spin sublevels in a magnetic field, and is closely related to the well-known "radical-pair" mechanism;[21,22] versions of this model were described in more details previously.[16,23] We note that the MEL(B) response isotope dependence can be also explained by the BP model.[11]

The basic PP spin Hamiltonian H_0 includes the Zeeman, HFI, and exchange terms:

$$H_0 = H_{\text{Zeeman}} + H_{\text{HF}} + H_{\text{ex}}. \tag{1}$$

In Eq. (1) H_{HF} is the HFI term,

$$H_{\text{HF}} = \sum_{i=1}^{2} \sum_{j=1}^{N_i} a_{ij} \vec{S} \cdot \vec{I}_{ij}, \tag{2}$$

where a_{ij} is the isotropic HFI describing the interaction between polaron spin S_i ($=\frac{1}{2}$) and N_i neighboring nuclei, each with spin I_{ij}. For protons in organic molecules the HFI constant is of the order of $a(\text{H}) \sim 0.3$ μeV (or $a/g\mu_B \sim 3$ mT).[13] The electronic Zeeman interaction term in Eq. (1) is

$$H_{\text{Zeeman}} = \mu_B (g_1 \vec{S}_1 + g_2 \vec{S}_2) \cdot \vec{B}, \tag{3}$$

where g_i ($\sim$2) is the respective g factor of each of the polarons in the PP species, and μ_B is the Bohr magneton. Finally the exchange interaction is written as

$$H_{\text{ex}} = 2\mu_B B_{\text{ex}} \vec{S}_1 \cdot \vec{S}_2 , \tag{4}$$

where B_{ex} measures the strength of the exchange interaction (we chose here for simplicity scalar HFI, g factors, and exchange interaction). In the absence of the spin orbit interaction the configuration space of H_0 is of dimension $M = 4\prod_{i=1}^{2}\prod_{j=1}^{N_i}(2I_{ij}+1)$. We did not specifically include the spin-orbit interaction in Eq. (1), but it could in principle be calculated for the Alq_3 molecule.

When the MEL (and/or MC) response originates from spin mixing within the PP species, then it is controlled by the relative PP singlet and triplet fractions, and their spin dependent decay processes such as fusion into excitons or dissociation into free charges. These decay processes are not contained in the spin Hamiltonian, Eq. (1) as H_0 is an Hermitian operator that conserves energy. A convenient way to include the spin dependent decay kinetics is to add to H_0 a non-Hermitian decay (relaxation) term:[22,24]

$$H_R = -\frac{i\hbar}{2} \sum_{\alpha} \gamma_\alpha P^\alpha , \tag{5}$$

where α designates the four singlet and triplet states: namely $\alpha = S, T_0, T_{\pm 1}$; and P^α and γ_α are the state projection operator and decay rate constant, respectively. The time evolution of the decaying density operator is now expressed in terms of the total Hamiltonian, $H = H_0 + H_R$,

$$\sigma(t) = \exp(-iHt/\hbar)\sigma^0 \exp(iH^\dagger t/\hbar) , \tag{6}$$

where $H^\dagger$ is the Hermitian conjugate of H, and the $t = 0$ density matrix σ^0 is determined by the PP generation process. The time evolution of the singlet and triplet PP fraction may now be written as

$$\begin{aligned} \rho_\alpha(t) &= \text{Tr}[P^\alpha \sigma(t)] \\ &= \frac{4}{M} \sum_{n,m} P^\alpha_{n,m} \sigma^0_{nm} \cos(\omega_{mn} t) \exp(-\gamma_{mn} t) , \end{aligned} \tag{7}$$

where $E_n = \hbar(\omega_n - i\gamma_n)$ are the (complex) eigenvalues of H, $\omega_{nm} = \omega_n - \omega_m$; $\gamma_{nm} = \gamma_n + \gamma_m$ the double summation (n,m) is over all M states. Equation (7) expresses the fact that the PP singlet (or triplet) time evolution contains both a coherent character [through the $\cos(\omega_{mn}t)$ factor] and an exponential decay factor. The measured MFE (that is MC and MEL) may directly be calculated using Eq. (7). The final expression for the MEL response depends on the radiative recombination of the SE and the detailed relaxation route from PP to form SE. We denote the effective SE generation rate from the PP^α configuration by $k_{\alpha,\text{SE}}$. Consequently, we define the "SE generation yield" $\Phi_{\text{SE}} = \sum_\alpha \Phi_{\alpha,\text{SE}}$, where $\Phi_{\alpha,\text{SE}}$ is given by

$$\Phi_{\alpha,\text{SE}} = \int_0^\infty k_{\alpha,\text{SE}} \rho_\alpha(t) dt = \frac{4}{M} \sum_{n,m} P^\alpha_{n,m} \sigma^0_{mn}(0) \frac{k_{\alpha,\text{SE}} \gamma_{nm}}{\gamma_{nm}^2 + \omega_{nm}^2} . \tag{8}$$

The contribution of the PP mechanism to the MEL(B) response is then given by

$$\text{MEL}_{\text{PP}}(B) = \frac{\Phi_{\text{SE}}(B) - \Phi_{\text{SE}}(0)}{\Phi_{\text{SE}}(0)} . \tag{9}$$

In Figs. 5(a) and 5(b) we show the simulated MEL_{PP} response, using Eq. (9) for two HFI cases (i) H-Alq_3 with $I = \frac{1}{2}$ and $a_{\text{HF}}/g\mu_B = 4$ mT; and (ii) D-Alq_3 with $I = 1$ and $a_{\text{HF}}/g\mu_B = 0.6$ mT. In both cases we chose $B_{\text{ex}} = 0.2$ mT. Comparing the simulation to the MEL data presented in Figs. 3(b) and 3(c) we conclude that the isotope dependent width and USMFE minima are captured by the PP mechanism with the HFI as the main spin mixing process.

B. Collision of spin $\frac{1}{2}$ polaron with triplet-state polaron-pair: Low field MC response

Unlike the MEL response discussed above, the obtained MC(B) response does not show much isotope effect due to HFI, indicating the dominance of a different spin mixing mechanism. In this section we introduce a novel, isotope insensitive mechanism that affects the MC response but does not affect the MEL response. That the MEL and MC responses are not similar to each other in Alq_3 was recently measured and discussed.[25]

The many PP that are produced from the injected free carriers do not have a fixed interpolaron distance d_P, but rather form a distribution of d_P. As the PP fuse to form excitons, d_P gradually decreases while the singlet and triplet states PP, namely PP_S and PP_T, separate in energy until the appropriate values for the SE and TE in the material are reached. In the intermediate state, where spin mixing between PP_S and PP_T is already diminished due to their large energy separation, PP_T still evolves with B because of its nonzero spin. Also PP_T may interact with spin $\frac{1}{2}$ carriers via magnetic spin-spin interaction. Such an interaction may be described by a "collision process" in which a spin $\frac{1}{2}$ carrier ("polaron") is temporarily paired with a close PP_T neighbor which causes magnetic field dependent carrier density that generates a finite MC(B) response. This mechanism does not contribute to MEL, and is insensitive to isotope exchange. The contribution to MC(B) comes from the direct PP_T dissociation, thus leading to isotope independent MC response. Similar triplet-doublet interaction has been considered before in connection with TE quenching by free radicals,[26] as well as for mobilization of trapped charge carriers in molecular crystals.[27]

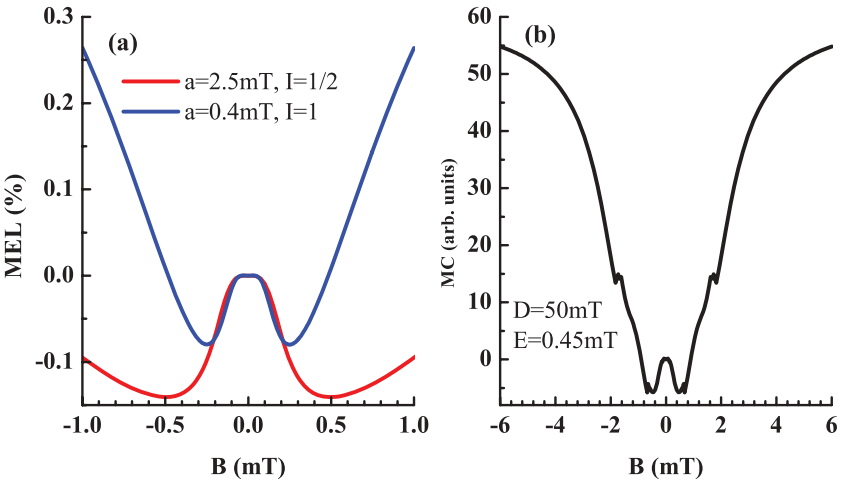

FIG. 5. (Color online) Model simulation for the low field MEL and MC responses of Alq_3. (a) PP mechanism for MEL(B) of H- and D-Alq_3: red line, $a/g\mu_B = 2.5$ mT, $I = \frac{1}{2}$ (H); blue line, $a/g\mu_B = 0.4$ mT, $I = 1$ (D). A finite exchange interaction of strength $B_{ex} = 0.02$ mT was used for both responses. (b) Polaron/PP_T scattering model for the isotope independent MC(B). The line shown was calculated using the zero-splitting parameters $D_P/g\mu_B = 50$ mT and $E_P/g\mu_B = 0.45$ mT in the triplet spin Hamiltonian.

Similar to the triplet-doublet collision model,[26] we envision the carrier-PP collision event as a process by which the $S_1 = 1$ PP_T and $S_2 = \frac{1}{2}$ charge carrier are temporarily paired together (forming a $PP_T - P$ pair), which evolves with time in a magnetic field, and then dissociates into free carrier and PP_T, respectively. The $PP_T - P$ species may be either in a quartet ($S = S_1 + S_2 = 3/2$) or doublet ($S = S_1 - S_2 = \frac{1}{2}$) spin states. The PP_T-P species spin Hamiltonian in a magnetic field may be written as

$$H_P = H_{PP_T} + J_P \vec{S}_1 \cdot \vec{S}_2 + H_Z + H_R, \tag{10}$$

where H_Z is the Zeeman energy term given by Eq. (3) with g_1 (g_2) as the PP_T (free carrier) g factor, J_P is the $PP_T - P$ spin-spin interaction constant, and H_{PP_T} is the PP_T triplet spin Hamiltonian term given by

$$H_{PP_T} = \vec{S}_1 \cdot \tilde{\tau} \cdot \vec{S}_1, \tag{11}$$

where $S_1 = 1$ is the PP_T spin and $\tilde{\tau}$ is the triplet[28] symmetric traceless tensor of rank 2. In the triplet principal reference frame: $H_{PP_T} = D_P(S_{1z}^2 - 2/3) + E_P(S_{1x}^2 - S_{1y}^2)$, where D_P and E_P are referred to as the PP_T zero field splitting (ZFS) parameters. The decay of the quartet and doublet states (with decay constants γ_{Qr} and γ_{Db}, respectively) is represented by the non-Hermitian relaxation term[22,24] H_R in Eq. (10), similar to Eq. (5). Following the procedure outlined in Sec. IV A above we may now calculate the magnetic field dependent density of free polarons that dissociate out of the $PP_T - P$ pairs. Denoting the dissociation rate from the $(PP_T - P)^\alpha$ (α = quartet, doublet) configuration by d_α, the free polaron yield and its contribution to MC are given by Eqs. (8) and (9), with d_α in place of $k_{\alpha,SE}$. The decay and dissociation constants (γ_α and d_α) determine mainly the magnitude of the MFE, whereas the triplet parameters D_P and E_P determine the overall width and the behavior at low fields (for $E_P \ll D_P$), respectively. In Fig. 5(b) we show a simulated MC(B) response for $D_P/g\mu_B = 50$ mT and $E_P/g\mu_B = 0.45$ mT. The simulated response is isotope insensitive, and features the sign change and minimum at $B < 1$ mT as in the experiment [Fig. 3(f)]. It is important to note that in addition to this proposed mechanism, other triplet based mechanisms (e.g., polaron collision with TE) exist in the literature, and may be also responsible for the high field MFE response.

V. SUMMARY

Using the spin $\frac{1}{2}$ CDMR and MR_{sv} in OSV devices based on H- and D-Alq_3 we showed that the HFI is indeed a significant spin relaxation mechanism for spin $\frac{1}{2}$ polarons in Alq_3. Moreover, the HFI provides an important spin mixing mechanism for polaron pairs in Alq_3 that may explain the MEL(B) response. The reduced HFI in D-Alq_3 with respect to H-Alq_3 is clearly observed in a variety of spin $\frac{1}{2}$ related experiments. We obtained: (a) narrower spin $\frac{1}{2}$ CDMR resonance line in D-Alq_3; (b) longer spin diffusion length in OSV based on D-Alq_3; (c) narrower MEL(B) response and smaller B_m in OLEDs based on D-Alq_3. In contrast, the MC(B) response is much less sensitive to isotope exchange and thus the HFI-based spin mixing mechanism here is overwhelmed by another, isotope insensitive spin mixing mechanism. To explain the low field behavior of MC in Alq_3 we offer an isotope independent interaction between free carrier with $S = \frac{1}{2}$ and triplet-state PP.

ACKNOWLEDGMENTS

Y.J.P. would like to thank Taiyo Nippon Sanso Corp. for providing the deuterated ingredients for the synthesis of deuterated Alq_3. This work was supported in part by the NSF (Grant No. DMR-1104495 and MRSEC program (DMR-1121252) at the UoU; T.D.N. and Z.V.V.); the Israel Science Foundation (ISF 472/11; E.E.), the US-Israel BSF (Grant No. 2010135; Z.V.V. and E.E.), and the NSFC and NBRPC (Grant No. 2012CB922003, X.G.L.).

*Corresponding author: val@physics.utah.edu

[1] C. W. Tang and S. A. VanSlyke, Appl. Phys. Lett. **51**, 913 (1987).
[2] C. W. Tang, S. A. VanSlyke, and C. H. Chen, J. Appl. Phys. **65**, 3610 (1989).
[3] W. Li, R. A. Jones, S. C. Allen, J. C. Heikenfeld, and A. J. Steckl, J. Display Technol. **2**, 143 (2006).
[4] J. Kalinowski, M. Cocchi, D. Virgili, P. Di Marco, and V. Fattori, Chem. Phys. Lett. **380**, 710 (2003).

[5]O. Mermer, G. Veeraraghavan, T. L. Francis, Y. Sheng, D. T. Nguyen, M. Wohlgenannt, A. Kohler, M. K. Al-Suti, and M. S. Khan, Phys. Rev. B **72**, 205202 (2005).
[6]Y. Sheng, T. D. Nguyen, G. Veeraraghavan, O. Mermer, M. Wohlgenannt, S. Qiu, and U. Scherf, Phys. Rev. B **74**, 045213 (2006).
[7]C. Gärditz, A. G. Mückl, and M. Cölle, J. Appl. Phys. **98**, 104507 (2005).
[8]P. Desai, P. Shakya, T. Kreouzis, W. P. Gillin, N. A. Morley, and M. R. J. Gibbs, Phys. Rev. B **75**, 094423 (2007).
[9]N. J. Rolfe, M. Heeney, P. B. Wyatt, A. J. Drew, T. Kreouzis, and W. P. Gillin, Phys. Rev. B **80**, 241201(R) (2009).
[10]J. A. Gómez, F. Nüesch, L. Zuppiroli, and C. F. O. Graeff, Synth. Met. **160**, 317 (2010).
[11]P. A. Bobbert, T. D. Nguyen, F. W. A. v. Oost, B. Koopmans, and M. Wohlgenannt, Phys. Rev. Lett. **99**, 216801 (2007).
[12]B. Koopmans, W. Wagemans, F. L. Bloom, P. A. Bobbert, M. Kemerink, and M. Wohlgenannt, Philos. Trans. R. Soc. London Sect. A **369**, 3602 (2011).
[13]A. Carrington and A. D. McLachlan, *Introduction to Magnetic Resonance* (Harper and Row, New York, 1967).
[14]N. J. Rolfe, M. Heeney, P. B. Wyatt, A. J. Drew, T. Kreouzis, and W. P. Gillin, Synth. Met. **161**, 608 (2011).
[15]T. D. Nguyen, B. R. Gautam, E. Ehrenfreund, and Z. V. Vardeny, Phys. Rev. Lett. **105**, 166804 (2010).
[16]T. D. Nguyen, G. Hukic-Markosian, F. J. Wang, L. Wojcik, X. G. Li, E. Ehrenfreund, and Z. V. Vardeny, Nat. Mater. **9**, 345 (2010).
[17]C. C. Tong and K. C. Hwang, J. Phys. Chem. C **111**, 3490 (2007).
[18]F. Wang, C. G. Yang, E. Ehrenfreund, and Z. V. Vardeny, Synth. Met. **160**, 297 (2010).
[19]M. Cölle, C. Gärditz, and M. Braun, J. Appl. Phys. **96**, 6133 (2004).
[20]H. D. Burrows, M. Fernandes, J. S. de-Melo, A. P. Monkman, and S. Navaratnam, J. Am. Chem. Soc. **125**, 15310 (2003).
[21]H. Hayashi, *Introduction to Dynamic Spin Chemistry; Magnetic Field Effects on Chemical and Biochemical Reactions* (World Scientific, Singapore, 2004).
[22]C. R. Timmel, U. Till, B. Brocklehurst, K. A. McLauchlan, and P. J. Hore, Mol. Phys. **95**, 71 (1998).
[23]E. Ehrenfreund and Z. V. Vardeny, Isr. J. Chem. **52** (2012).
[24]J. Tang and J. R. Norris, Chem. Phys. Lett. **92**, 136 (1982).
[25]A. Buchschuster, T. D. Schmidt, and W. Brutting, Appl. Phys. Lett. **100**, 123302 (2012).
[26]V. Ern and R. E. Merrifield, Phys. Rev. Lett. **21**, 609 (1968).
[27]U. E. Steiner and T. Ulrich, Chem. Rev. **89**, 51 (1989).
[28]A. Abragam and B. Bleaney, *Electron Paramagnetic Resonance of Transition Ions* (Clarendon, Oxford, 1970).